ESTIMATION OF DEFOCUS AND ASTIGMATISM IN TRANSMISSION ELECTRON MICROSCOPY

M.Vulović[1,2], P.L.Brandt[1], R.B.G.Ravelli[2], A.J.Koster[2], L.J.van Vliet[1] and B.Rieger[1,3]

1. Quantitative Imaging Group, TU Delft, Lorentzweg 1, 2628 CJ Delft, The Netherlands
2. Molecular Cell Biology, LUMC, Einthovenweg 20, 2333 ZC Leiden, The Netherlands
3. FEI Company, Achtseweg Noord 5, 5651 GG Eindhoven, The Netherlands

ABSTRACT

Image formation in phase-contrast electron microscopy is governed by the contrast transfer function (CTF). The key parameter to tune the CTF is the defocus. A precise and unbiased estimate of the defocus is essential to determine the forward model and interpret high resolution images in cryo-TEM. We present an algorithm based on the weak-phase approximation for determination of the defocus and astigmatism of the objective lens from recorded images of an amorphous sample. The algorithm identifies Thon rings in the power spectrum density (PSD) and uses them to estimate astigmatism and defocus together with their uncertainties. For the astigmatism estimation we use a transformation to polar coordinates to fit ellipses to the Thon rings. Averaging the PSD over these ellipses reduces CTF estimation to a 1D problem and enhances the signal-to-noise ratio.

Index Terms— cryo-TEM, phase contrast, CTF estimation, astigmatism

1. INTRODUCTION

Electron microscopy is the only technique available to determine the 3D structures of large macromolecular complexes that resist crystallization attempts. In order to obtain near-atomic resolution it is essential to incorporate the effects of the contrast transfer function (CTF) of the microscope, the elastic and inelastic scattering properties of the sample and the effects of the TEM detector on the computed 3D reconstruction of the macromolecular complex. Determination of the CTF parameters, especially defocus, is crucial in designing filtering strategies to account for the effect of the CTF and for interpretation of the images for spatial frequencies beyond the first zero-crossing of the CTF. Several programs for the estimation of CTF parameters have been developed. A survey of some freely available algorithms and some crucial papers regarding defocus estimation can be found in [1] and [2]. In order to enhance the signal-to-noise ratio (SNR) of the power spectrum density (PSD) rotational or periodogram averaging is commonly performed. We apply elliptical or angular averaging and robust minima detection to the PSD. The robustness of the defocus estimation and its uncertainties are of great importance. This paper describes and analyzes an algorithm to automatically estimate defocus and astigmatism together with corresponding uncertainties. False minima in the spectrum are recognized and ignored. Simulations are performed to compare our method against ACE toolbox [1], one of the state of the art programs for automatic CTF estimation that is commonly used. We evaluate the robustness of the estimate on experimental data by repeating measurements at identical TEM imaging conditions.

2. THEORY

In the first approximation, image formation in the electron microscope can be considered as a linear process. For non-tilted and thin specimens, the defocus is constant across the field of view and therefore, the CTF and envelopes are spatially invariant. Phase contrast occurs as a result of interference between the elastically scattered electrons from the specimen and the unaffected beam. These electrons are further subjected to a frequency dependent phase shift introduced by microscope aberrations [3]

$$\phi\left(q^*\right) = 2\pi\left(1/4q^{*4} - 1/2\Delta f^* q^{*2}\right) \quad (1)$$

with $q^* \equiv q\sqrt[4]{C_s\lambda^3}$, $\Delta f^* \equiv \Delta f\sqrt{(C_s\lambda)^{-1}}$, q the spatial frequency, C_s the spherical aberration, λ the electron wavelength, and Δf the defocus. The oscillating part of the CTF is $T_\phi(q) = \cos\left(\phi(q)\right) - i\sin\left(\phi(q)\right)$. For weak phase objects in the absence of amplitude contrast, only the imaginary term remains. The energy spread and the finite size of the source introduce temporal and spatial incoherence and can respectively be modeled as damping envelopes K_c and K_s in the spatial frequency domain. The total CTF is then

$$T(q) = T_\phi(q)K_c(q)K_s(q). \quad (2)$$

The observed contrast is minimal when the CTF is zero. That occurs for zeros of the sine term

$$2\pi\left(q_0^{*4}/4 - q_0^{*2}\Delta f^*/2\right) = k\pi. \quad (3)$$

The location of the zeros depends on the defocus, the accelerating voltage and the spherical aberration.

3. ESTIMATION OF THE DEFOCUS AND ASTIGMATISM FROM THON RINGS

In order to estimate the CTF, the sample properties must be known. For that purpose the most convenient phase specimens are amorphous films. It is assumed that they produce a noisy signal with a flat frequency response. Figure 1 displays the PSD of a recorded image of PtIr (platinum-iridium) showing a pattern referred to as Thon rings. Angular averaging applied to the quantity $P = |\mathcal{F}\{\sqrt{I} - \langle\sqrt{I}\rangle\}|^2$ yields a 1D (radial) PSD, where $\langle\bullet\rangle$ denotes spatial averaging, F the Fourier transform and I the intensity image. Angular averaging of the PSD was performed by computing the weighted average inside rings with a Gaussian profile $G(r,\sigma)$. The resulting radial PSD yields the enhanced Thon rings; the minima in the PSD correspond to the zeros of eq. (3). After averaging, a model for the inelastic background was fitted through the minima of the radial PSD and subtracted from it. In the presence of astigmatism the averaging was done along ellipses.. Therefore, the parameters of the ellipses fitted through the minima of the PSD needed to be determined first.

3.1. Astigmatism determination

The shape of the Thon rings in the PSD is circular if there is no astigmatism present. In the case of twofold astigmatism, however, the total phase shift has an angular dependency $\phi(q,\alpha) = 2\pi\left(\frac{1}{4}C_s\lambda^3 q^4 - \frac{1}{2}\lambda q^2\left(\Delta f - A_1\cos\left(2\left(\alpha-\alpha_1\right)\right)\right)\right)$. Whereas the q^4 term is isotropic, the q^2 term is not and has directional dependency. It is assumed here that amount of astigmatism is not excessive so PSD contains elliptical equi-phase contours. The astigmatism was determined from the minima of the 2D PSD in the radial direction. The positions of the minima are presented in the polar coordinate system (Figure 7a) and were segmented based upon the radius and a measure for strength of each minima (Figure 7b). This measure is defined as the ratio of the distance between the two surrounding maxima and their average height. For each elliptical ring, the ratio between the

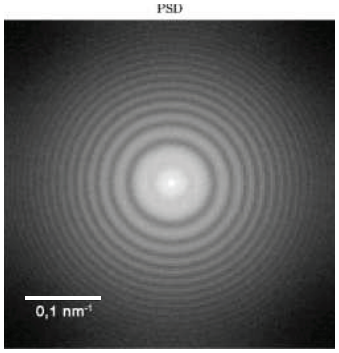

Figure 1. The power spectrum density of an image of PtIr acquired on a FEI Titan Krios; 500k magnification; defocus 1µm

major and minor axes (R) was found with corresponding orientation α_1. Two-fold astigmatism was then computed as $A_1 = \Delta f(R^2-1)/(R^2+1)$. Furthermore, P was averaged over the elliptical Gaussian rings to yield a 1D PSD.

3.2. Defocus determination (k-trajectory method)

After performing elliptical or angular (in a case of negligible astigmatism) averaging and after subtraction of the background, the local minima of the resulting curve were used to estimate the defocus. These minima correspond to the minima of the CTF^2 (zero crossings of the CTF). The radial sin^2-term for various amounts of defocus with positions of the minima and maxima superimposed is shown in Figure 2. It can be seen that the contrast transfer is poor at zero defocus. Following the q-axis direction, first a wide region of low contrast is encountered. In overfocus ($\Delta f^* < 0$) contrast improves, but the pass band is small and minima are quickly encountered. In underfocus ($\Delta f^* > 0$) there are the interesting regions where the maxima curves (green lines) are vertical. In this region the contrast transfer is high for a wide frequency band. The zero-crossings condition of the CTF (3) can be used to solve for the defocus of each individual zero crossing i as:

$$\Delta f_i = (C_s\lambda^3 q_{0,i}^4 - 2k_i)/(2\lambda q_{0,i}^2) \qquad (4)$$

The problem we face now is: which k_i corresponds to the frequency $q_{0,i}$. Considering a negative defocus in Figure 2, the i-th zero-crossing corresponds to $k = i$. However, considering a positive defocus, in the first region $q^*_{0,i=1}$ corresponds again to $k = 0$, but $q^*_{0,i}$ $(i > 1)$ corresponds to $k = i$-1. For an underfocus larger than $2^{1/2}$, the positive k values are encountered. For each k-sequence the values of Δf_i can be calculated using eq. (4). The k-sequence for which Δf_i has the smallest variance is assumed to be the correct one. The average over all Δf_i is the estimate of the actual defocus.

There are cases, for relatively small defocus values, when minima in the CTF^2 do not correspond to a zero crossing in the CTF. They might be falsely detected as zero crossings, hampering the k-trajectory method. This is illustrated in Figure 3. The envelopes of the CTF were excluded from analysis since they do not change the position of zeros. The blue line represents a simulated CTF^2 for $\Delta f^* = 1.9$, and the corresponding k-trajectory (c.f. Figure 2) is k = 0,-1,-1,0,1,2, etc. At this defocus value, an additional minimum occurs which is not a zero-crossing of the CTF. In Figure 3, the red line shows the CTF^2 and the defocus estimate when all minima are used including the false one (k = 0,-1,-2,-1,0,1, etc.). This minimum causes a slight error in the defocus estimate. We allow one of the local minima not to be a zero crossing; repeat this for all found minima and chose the k-trajectory with the smallest overall variance.

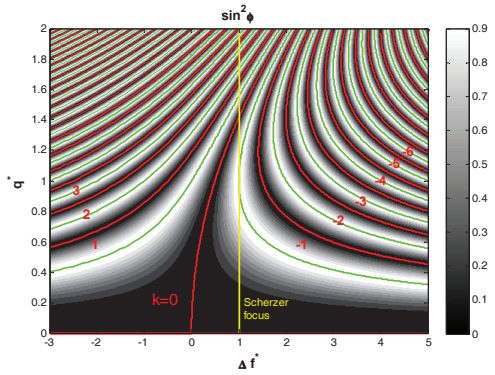

Figure 2. The square of the oscillating part of the CTF. The red and the green lines indicate minima (and k) and maxima respectively.

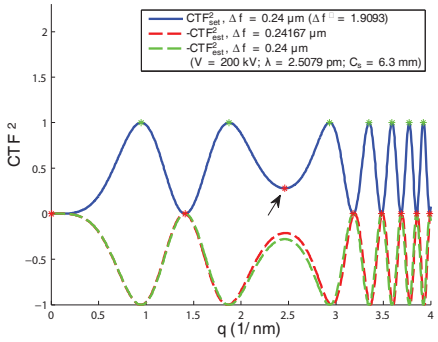

Figure 3. An illustration of the flaw due to a local minimum which is not a zero crossing of the CTF. The blue line shows the simulated CTF^2 at $\Delta f^* = 1.9$. The red and the green lines show CTF^2 estimates with and without additional minimum, respectively. The additional minimum is indicated by the black arrow. The CTF^2 curve is flipped for the better visualization

4. RESULTS

4.1. Validation by simulations

For amorphous material the imaged structure results effectively in white noise. Therefore, the test signal of weak phase objects can be modeled by a constant amplitude A_0 as the real part and Gaussian distributed noise $G(\sigma_e)$ (A_0 » $G(\sigma_e)$) as the imaginary part. The envelopes of the CTF and the background of the PSD were modeled according to [3]. Our method was tested on 99 test images and compared to an algorithm which is implemented in the ACE toolbox [1]. The defocus was set to 1 µm and the ACE estimate was ~5 % off (Figure 4a). However, it was very precise for 65 out of 99 test images. Since our method can calculate the defocus for each minimum separately, histograms for the first 8 minima are presented in Figure 4b, as well as mean defocus from all minima (average defocus). We found very good agreement between the simulated and estimated defocus (less than 0.1%) and the spread of the estimate was also very small (less than 1nm). From the histograms, we observe that the central zero-crossings have smaller spread than the low and high frequency ones. Inelastic background is dominant at low frequencies and hampers the accuracy of the minimum determination. Detection of the high frequency minima becomes less accurate due to the lower SNR.

4.2. Measurements

Figure 5 shows the estimation of defocus from the recorded image presented in Figure 1. The estimated defocus deviates slightly from the set defocus. However, the very small standard deviation of the fit illustrates its precision; 26 zeros were accurately determined. The robustness of the algorithm was also tested by imaging carbon (C-flat) 30 times at three different nominal defoci (Figure 6). The difference (bias) between estimated and set defocus was around 50nm. The defocus estimate for 1 μm set defocus was not stable due to the drift of the specimen. For the two stable defoci (1.25 μm and 1.5 μm), the spread in the consecutive defocus estimates (Figure 6., right) is smaller than the individual uncertainties (gray area). Furthermore, the advantage of using elliptical instead of circular averaging of the PSD of an astigmatic image is shown in Figure 7. The values for the astigmatism were compared with the values obtained from the commercially available package Digital Micrograph (www.gatan.com/software/) and were similar within a few percent if we only fit ellipses to the first two rings. If we include high frequencies ellipses the discrepancy was ~10%.

5. DISCUSSION AND CONCLUSION

We have presented an algorithm for the accurate and precise estimation of defocus and astigmatism from the PSD of images of amorphous specimens. In addition, it provides an estimate of the uncertainty in the estimated defocus and automatically discards a false zero-crossing of the CTF that occurs for low defocus values. Simulations have shown the robustness of the method (a spread less than 0.1%). Our model for the envelope and the inelastic background (Lorentzian function) is based on a theoretical model [3], whereas the ACE toolbox introduces an empirical approach. This might be one of the reasons for the discrepancy between the result of our method and that of the ACE toolbox. It can be seen from the histograms in Figure 4 that some minima are more reliable (small spread in defocus) than others. In practice, spread of individual minima could be determined only by taking a large number of images with certain settings of the microscope. The spread can be further used to weight the influence of each zero in the defocus estimation and may lead to a more precise estimate. The uncertainty of the defocus estimation from one image depends on the number of zeros detected, but as shown in Figure 6 the spread from repeated acquisitions and defocus estimates is smaller than the predicted uncertainty from an individual image. Furthermore, in order to estimate

astigmatism, parameters of the ellipses were extracted from the minima in the PSD rather than from edge detection (as implemented in ACE) since minima are less dependent on envelopes and background. The presence of a background due to inelastic scattering could introduce changes of the gradients in the PSD curve. Most of the algorithms developed so far (including ours) base their defocus estimation on the position of one or more minimum in the PSD. This becomes quite a challenging task when the specimen is embedded in vitreous ice as the SNR decreases by a factor of 10. One of the problems encountered is the estimation of the background which masks the CTF oscillations. In order to avoid fitting of the background

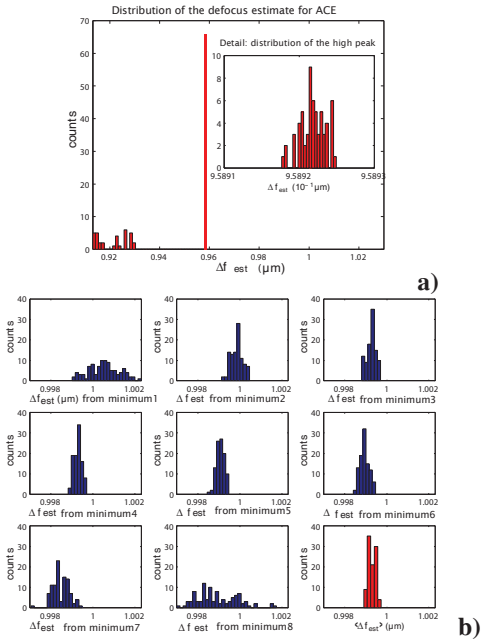

Figure 4. The histograms show the estimated defocus for a set defocus of 1μm. Each histogram is based on 99 test images; a) estimated by ACE toolbox b) estimated by k-trajectory method. The first eight images show the estimates for the separate minima and the ninth from all minima together.

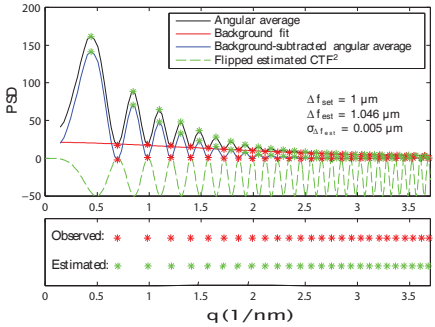

Figure 5. A k-trajectory CTF fit on an image showed in figure 1. The given standard deviation is calculated from the set of defocus estimates from the individual minima. Below, for the comparison, the observed zeros are plotted together with zeros of the CTF.

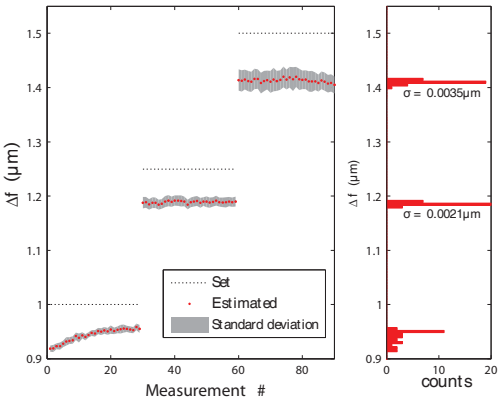

Figure 6. A series of measurements at three consecutively levels of defocus: 1 μm, 1.25 μm and 1.5 μm. The grey area represents the uncertainty given by the standard derivation of the defocus estimates for each zero-crossing in a single image. The right sub-image shows the distribution of the estimated defoci.

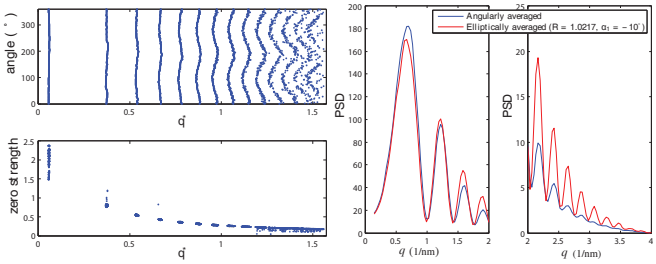

Figure 7. Left: a) positions of minima in polar representation of a 2D PSD and b) their corresponding 'strengths'. Right: The angular and elliptical average of a PSD. The y-axis of the image on the right is scaled

through the minima, Xiong *et al.*[2] estimate the background from images collected without any sample and combine periodogram averaging with rotational averaging. It is questionable whether this model properly describes the inelastic background for low spatial frequencies. In this region accurate background subtraction is important for extraction of the minima. The challenge remains how to accurately measure the defocus (at each location) of the non-tilted and tilted specimen embedded in vitreous ice.

6. REFERENCES

[1] S.P. Mallick, B. Carragher, C.S. Potter and D.J. Kriegman, "ACE: Automated CTF Estimation," *Ultramicroscopy*, Elsevier, pp. 8-29, August 2005 .

[2] Q. Xiong, M. K. Morphew, C.L. Schwartz, A.H. Hoenger and D.N. Mastronade "CTF Determination and Correction for Low Dose Tomographic Tilt Series," *Journal of Structural Biology*, Elsevier, pp. 378-387, December 2009.

[3] Reimer, L., *Transmission Electron Microscopy*, Springer-Verlag, Berlin, 1984.